

2009

# Gallium nitride sensors for hydrogen/nitrogen and hydrogen/carbon monoxide gas mixtures

Christopher Nicholas Monteparo  
*University of South Florida*

Follow this and additional works at: <http://scholarcommons.usf.edu/etd>

 Part of the [American Studies Commons](#)

---

## Scholar Commons Citation

Monteparo, Christopher Nicholas, "Gallium nitride sensors for hydrogen/nitrogen and hydrogen/carbon monoxide gas mixtures" (2009). *Graduate Theses and Dissertations*.  
<http://scholarcommons.usf.edu/etd/2112>

This Thesis is brought to you for free and open access by the Graduate School at Scholar Commons. It has been accepted for inclusion in Graduate Theses and Dissertations by an authorized administrator of Scholar Commons. For more information, please contact [scholarcommons@usf.edu](mailto:scholarcommons@usf.edu).

Gallium Nitride Sensors for Hydrogen/Nitrogen and Hydrogen/Carbon Monoxide Gas  
Mixtures

by

Christopher Nicholas Monteparo

A thesis submitted in partial fulfillment  
of the requirements for the degree of  
Master of Science in Chemical Engineering  
Department of Chemical and Biomedical Engineering  
College of Engineering  
University of South Florida

Major Professor: John T. Wolan, Ph.D.  
Venkat Bhethanabolta, Ph.D.  
Scott Campbell, Ph.D.  
Jeffrey Cunningham, Ph.D.

Date of Approval:  
March 6, 2009

Keywords: bandgap, resistive sensors, semiconductor, syn-gas, Fischer-Tropsch synthesis

© Copyright 2009, Christopher Nicholas Monteparo

## **Dedication**

This work is dedicated with love to my parents and grandparents.

Thank you for everything you have given me, especially the gift of knowledge and the  
spark of curiosity.

## **Acknowledgments**

This work is the culmination of ongoing research since my undergraduate years. Without the wisdom and guidance of others, I would not have been able to see it to completion. I would especially like to acknowledge Dr. John T. Wolan for his counsel and encouragement throughout my research and education. Also, I thank Dr. Carlos Smith and Mr. Charles Gimbel for establishing my interest in Chemical Engineering.

I would also like to acknowledge the foundations of my research put forth by Dr. Timothy Fawcett and Dr. Jodi Pope. I would like to thank Dr. Timothy Fawcett for following up on the project and providing invaluable assistance. I would also like to thank Dr. Hadis Morkoc for allowing me the use of the GaN sensors and Dr. Babu Joseph for his support of my research.

Over the years, I have had help from a variety of colleagues and friends in the Applied Surface Science Laboratory. Dr. Benjamin Grayson, Ala'a Kababji, Aaron Black, Brad Ridder, Phil Saraneeyavongse, and Ali Syed-Gardezi have been close friends and a great source of knowledge, experience, and camaraderie. I would also like to thank my fellow Master's Program students Alex Page and Patrick Brandon for their support and conviviality.

Finally, I would like to thank my family and friends for their faith and encouragement. I would especially like to thank Christine Bringes for her dedication and care for the last year and a half. Without them, I might have fallen down the quick and easy path. Instead, they encouraged me to do my best and reach new heights.

## Table of contents

List of tables .....	iii
List of figures .....	iv
Abstract .....	v
Chapter 1: Introduction .....	1
1.1 Motivation.....	1
1.2 Research objectives.....	2
1.3 Methodology .....	2
1.4 Expected contribution of the research.....	3
1.5 Thesis overview .....	3
Chapter 2: Hydrogen technology and detection.....	4
2.1 Hydrogen energy technologies .....	4
2.2 Hydrogen sensors.....	5
2.3 Summary .....	6
Chapter 3: Gallium nitride and semiconductor sensors .....	8
3.1 Applying gallium nitride properties to sensors .....	8
3.1.1 Bandgap structure of GaN.....	8
3.1.2 Thermal stability .....	10
3.1.3 Electron mobility.....	10
3.2 Comparison of semiconductor sensors .....	11
3.2.1 Gate sensors .....	12
3.2.2 MOS sensors .....	13
3.2.3 Schottky diode sensors.....	13
3.2.4 Resistive sensors .....	15
3.3 Summary .....	16
Chapter 4: Experimental methods.....	18
4.1 Gas sensor setup.....	18
4.2 Experimental procedures .....	20
Chapter 5: Data and analysis.....	22
5.1 Hydrogen detection in nitrogen at 200 °C and 300 °C .....	22
5.2 Sensor response to H <sub>2</sub> /CO mixtures.....	23

5.3 Relationship between sensor response and thermal conductivity.....	25
5.4 Summary .....	28
Chapter 6: Conclusions and future work .....	29
6.1 Conclusions .....	29
6.2 Future work .....	30
6.2.1 Further investigation into high temperature response.....	30
6.2.2 Further investigation of synthesis gas sensitivity .....	30
6.2.3 Further investigation of thermal property relationships.....	31
References .....	32
Appendices.....	36
Appendix A: Nomenclature .....	37

### **List of tables**

Table 2.1: Heating values of hydrogen and fossil fuels .....	5
Table 2.2: Properties of odorless gases .....	6
Table 3.1: Semiconductor bandgap properties.....	9
Table 3.2: Melting points of semiconductors.....	10
Table 3.3: Electron mobility of semiconductors.....	11
Table 3.4: Summary of semiconductor sensors .....	17
Table 4.1: H <sub>2</sub> :CO experiment flow rates.....	21

## List of figures

Figure 3.1: Bandgap energy transitions .....	9
Figure 3.2: Gate sensor mechanism .....	12
Figure 3.3: MOS sensor structure .....	13
Figure 3.4: Schottky diode sensor.....	14
Figure 3.5: GaN resistive sensor .....	15
Figure 4.1: Gas sensor setup .....	19
Figure 5.1: GaN sensor responses to H <sub>2</sub> in N <sub>2</sub> mixtures at 200 °C and 300 °C.....	22
Figure 5.2: GaN sensor responses to H <sub>2</sub> in CO mixtures at 50 °C.....	24
Figure 5.3: Thermal conductivity vs. current change for H <sub>2</sub> in N <sub>2</sub> mixtures .....	27
Figure 5.4: Thermal conductivity vs. current change for H <sub>2</sub> in CO mixtures at 50 °C.....	28

# **Gallium Nitride Sensors for Hydrogen/Nitrogen and Hydrogen/Carbon Monoxide Gas Mixtures**

Christopher Nicholas Monteparo

## **ABSTRACT**

As hydrogen is increasingly used as an energy carrier, gas sensors that can operate at high temperatures and in harsh environments are needed for fuel cell, aerospace, and automotive applications. The high temperature Fischer-Tropsch process also uses mixtures of hydrogen and carbon monoxide to generate synthetic fuels from non-fossil precursors. As the Fischer-Tropsch process depends upon particular gas mixtures to generate various fuels, a sensor which can determine the proper ratio of reactants is needed.

To this end, gallium nitride (GaN) has been used to fabricate a resistive gas sensor. GaN is a suitable semiconductor to be used in hydrogen because of a wide, direct bandgap and greater stability than many other semiconductors. Additionally, resistive sensors offer several advantages in design compared to other types of sensors. Response time of resistive sensors is faster than those of other semiconductor sensors because catalytic and diffusion steps are not part of the response mechanism. Instead, a thermal detection mechanism is employed in resistive sensors.

In this work, sensor response to changes in hydrogen concentration in nitrogen was measured at 200°C and 300°C. Sensor response was measured as change in current

from a reference response to pure nitrogen at each temperature under a constant 2.5 V bias. Isothermal operation was achieved by controlling sensor temperature and pre-heating gas mixtures. Sensitivity to concentration increased upon an increase in temperature. Additionally, sensor response to concentration changes of H<sub>2</sub> in CO at 50 °C was demonstrated. Sensors show similar responses to nitrogen and carbon monoxide mixtures, which have similar thermal properties. Using the thermal detection mechanism of the sensors, a correlation was shown between sensor response and a gas mixture thermal conductivity.

## Chapter 1: Introduction

### 1.1 Motivation

Hydrogen has generated interest as an environmentally clean alternative to fossil fuels. For instance, hydrogen ( $H_2$ ) has been used as fuel in jet aircrafts, and high-temperature fuel cells provided internal power to spacecrafts during the Apollo Program [1,2]. Additionally, the Fischer-Tropsch synthesis (FTS) process uses synthesis gas (syn-gas), composed of hydrogen and carbon monoxide, to generate hydrocarbon fuels [3]. Production of fuels from FTS is of note because fossil precursors are not required. The extreme conditions of these applications limit the materials which can be used for hydrogen detection.

Design and implementation of  $H_2$  gas sensors have been improved through use of semiconductors, which yield compact and simple devices. Sensor size is reduced through the use of thin film semiconductor layers which are formed on the microscale [4-6]. Transmission of electrical signals between these layers is influenced by exposure to hydrogen. Current and voltage characteristics of sensors can then be correlated with concentration. Hence, interfacing sensors with control systems is straightforward.

Not all semiconductors are suitable for use in gas detection. Physical properties, such as melting point, constrain the temperature range in which a material functions properly. Careful consideration of material attributes has led to the creation of gallium nitride sensors for  $H_2$  detection at elevated temperatures.

## 1.2 Research objectives

The objective of this research is to demonstrate the detection of hydrogen in nitrogen at elevated temperatures and the detection of H<sub>2</sub>:CO ratios in gas streams using gallium nitride (GaN) resistive gas sensors. Sensor responses to small and large changes in concentration were compared in the case of H<sub>2</sub>/N<sub>2</sub> mixtures. The ability of GaN sensors to distinguish between H<sub>2</sub>:CO ratios was investigated with simulated syn-gas compositions. Correlations between the collected data to thermal conductivity were also investigated.

## 1.3 Methodology

Resistive sensor responses were measured as current change from a baseline current response of pure N<sub>2</sub>. When voltage is constant, a current change is directly related to a resistance change. Sensitivity for resistive sensors is change in current, (I), divided by change in hydrogen concentration, (C<sub>H<sub>2</sub></sub>), shown in Equation 1.1.

$$\text{Sensitivity} = \frac{\Delta I}{\Delta C_{H_2}} \quad (\text{Eqn 1.1})$$

The sensitivity was investigated through analysis of sensor responses over a range of concentrations. Experiments consisted of sensor response to hydrogen-nitrogen mixtures that varied hydrogen concentration from 0-100% at temperatures of 200°C and 300°C. First, the response to concentrations of pure nitrogen (N<sub>2</sub>) and pure hydrogen (H<sub>2</sub>) flow rates were measured. Next, sensor response to 10-100% H<sub>2</sub> in N<sub>2</sub> were measured at 10% intervals with a N<sub>2</sub> purge between each interval to remove any adsorbed H<sub>2</sub>. Finally, response to 1-10% concentrations in 1% intervals with purge was recorded.

Production of different fuels requires control of H<sub>2</sub>/CO ratio [3]. Hydrogen and carbon monoxide gas mixtures were used to simulate common synthesis gas compositions used in FTS. Experiments were conducted at 50 °C to determine if the response of GaN resistive sensors is affected by the H<sub>2</sub>:CO composition.

#### 1.4 Expected contribution of the research

This research demonstrates the operation of GaN resistive sensors over a range of temperatures. Previous experiments have explored the response of GaN resistive sensors at a lower temperature [7]. The response of these sensors at temperatures above 200 °C demonstrates how sensor sensitivity is affected by temperature. An investigation into GaN sensor response to H<sub>2</sub>/CO mixtures was conducted for the first time. Sensor function as a thermal conductivity detector was investigated using empirical thermal conductivity calculations.

#### 1.5 Thesis overview

In order to assist the reader, this thesis is organized as follows. Chapter 2 explains background information on hydrogen technologies to establish the importance of hydrogen detection. Chapter 3 presents GaN properties which are incorporated into sensor design and compares resistive sensors to other semiconductor sensors. In Chapter 4, the sensor test bed and experimental procedure are explained. Chapter 5 presents data and results for experiments involving H<sub>2</sub>/N<sub>2</sub> mixtures at 200 °C and 300 °C and H<sub>2</sub>:CO at 50 °C. Finally, Chapter 6 presents conclusions and recommendations for future work.

## Chapter 2: Hydrogen technology and detection

### 2.1 Hydrogen energy technologies

Hydrogen is a viable replacement for non-renewable fossil fuels. Unlike petroleum,  $H_2$  is renewable via the electrolysis of water, acidification of metals, steam reforming of natural gas, dissociation of ammonia and gasification of biomass or coal [8,9]. Hydrogen is already used as an energy carrier in fields such as aerospace and automobiles [1,2,10-11].

The energy content of  $H_2$  is greater than that of many commonly used fossil fuels, including gasoline, as shown in Table 2.1. The lower heating value (LHV) and higher heating value (HHV) are measurements of the heat released from fuel combustion. Heating values of hydrogen are more than double that of gasoline on a weight basis. However, widespread use of  $H_2$  gas in automobiles is of limited practicality because conventional storage systems are highly pressurized and heavy[12].  $H_2$  liquefaction and porous-material impregnation are developing alternatives for hydrogen storage [14].

Hydrogen fuel cells offer several advantages over engines using hydrocarbon fuels. Since fuel cells are not heat engines, they are not limited by the Carnot efficiency. In addition, only water is produced instead of environmentally harmful byproducts, such as  $CO_2$ . Hydrogen is commonly used in fuel cells with operating temperatures from as low as  $100\text{ }^\circ\text{C}$  in polymer electrolyte membrane (PEM) fuel cells to higher than  $1000\text{ }^\circ\text{C}$  in solid oxide fuel cells (SOFC) [2].

Table 2.1: Heating values of hydrogen and fossil fuels. [14] HHV is the amount of heat that is discharged as a quantity of fuel at 25 °C is combusted and the products return to 25 °C accounting for the latent heat of water produced. LHV neglects heat from water recovery and any product cooling below 150 °C.

<i>Fuel</i>	<i>LHV(MJ/kg)</i>	<i>HHV (MJ/kg)</i>
Hydrogen	119.9	141.6
Gasoline	44.5	47.3
Diesel	42.5	44.8

Hydrogen can also be used to alleviate demand for fossil fuels. Fischer-Tropsch synthesis (FTS) reactions of H<sub>2</sub>/CO synthesis gas (syn-gas) create synthetic hydrocarbons [3]. The products of these reactions are a distribution of hydrocarbons determined by variables including feedstock composition, catalyst selection, and operating temperatures [3,15]. Process control can then be improved by employing H<sub>2</sub> sensors for measuring feedstock H<sub>2</sub>/CO ratios.

## 2.2 Hydrogen sensors

Detection of hydrogen gas without sensors is a difficult problem because hydrogen is odorless and colorless. The properties of hydrogen are compared to those of other gaseous species in Table 2.2. Other odorless gases can be laced with a foul smelling mercaptan, which diffuses with the gas to alert nearby users of leaks before conditions become dangerous. H<sub>2</sub> diffusivity is larger than any known mercaptan so conditions could become hazardous before the presence of a leak is known. Reliance on sensors is a necessary alternative and allows H<sub>2</sub> concentration to be quantified.

Table 2.2: Properties of odorless gases. [16, 17]

<i>Species</i>	<i>MW</i> (g/mol)	<i>D<sub>A-Air</sub></i> at 20 °C (cm <sup>2</sup> /s)
H <sub>2</sub>	2.016	0.611
N <sub>2</sub>	28.02	-----
O <sub>2</sub>	32.00	0.178
CO	28.01	0.208
CO <sub>2</sub>	44.01	0.138

H<sub>2</sub> sensors serve a variety of purposes in industrial processes. Leak detectors are important from safety concerns due to hydrogen's explosion limit of 4% to 75% in air [18,19]. Determination of hydrogen content in molten metal is used to control porosity caused by dissolved gas [20]. Growth of anaerobic bacteria is monitored by hydrogen sensors in biological processes [21]. Sensors are used to control stream compositions in chemical reactions such as biomass gasification, FTS, and fuel cell redox [22,3].

Processes requiring H<sub>2</sub> detection often take place under intense temperature and/or pressure, such as in industrial reactors, microbes, and outer space [22,23,2,10]. Proper material selection enables sensors to function in these harsh conditions. To that end, GaN has been chosen as an appropriate material for use in H<sub>2</sub> sensors operating at elevated temperatures.

### 2.3 Summary

Hydrogen as an energy carrier is an attractive alternative to fossil fuels because of greater energy content. Fuel cells use hydrogen as a fuel to generate power more efficiently than combustion engines. The Fischer-Tropsch process uses hydrogen to create synthetic hydrocarbons which alleviates demand for fossil fuels. Safe control of

processes such as these requires hydrogen sensors. Sensor operating conditions are diverse. Selection of sensor materials needs to integrate operating variables into sensor design.

## **Chapter 3: Gallium nitride and semiconductor sensors**

### 3.1 Applying gallium nitride properties to sensors

The electrical and mechanical properties of GaN make it a suitable material for hydrogen sensing. GaN sensors are able to function at higher temperatures because GaN has a high melting point and a wide, direct bandgap. Fabrication of GaN resistive sensors is more economical than many other sensors because of inexpensive materials and a reduced number of processing steps.

#### 3.1.1 Bandgap structure of GaN

GaN has a wide bandgap compared to other semiconductors, as shown in Table 3.1, which allows sensor operation at higher temperatures. Electrons occupy different energy bands within semiconductors. The bandgap energy ( $E_g$ ) is the energy difference, in eV, between the valence and conduction bands of a semiconductor [24,25]. The bandgap is also called the forbidden gap because electrons cannot occupy the energy states within this region [24,25]. The band structure of semiconductors creates unique properties different from metals and insulators. Two classifications exist for semiconductor bandgaps, direct and indirect, based on whether electron momentum changes between the conduction and valence bands [25].

Table 3.1: Semiconductor bandgap properties. [25]

<i>Material</i>	$E_g$ (eV)	<i>Type</i>
GaN	3.42	Direct
Si	1.1	Indirect
SiC( $\alpha$ )	2.86	Indirect
GaP	2.26	Indirect
GaAs	1.43	Direct

Due to the direct bandgap of GaN, electron transition between energy levels does not require a change in momentum, yielding better energy absorption. Wave functions ( $\psi$ ) mathematically describe the electron wave properties, such as the direction of wave propagation called wave vector ( $k_\psi$ ). Figure 3.1 shows that there is a change in  $k_\psi$  of electrons transitioning from the valance to conduction band of indirect bandgap, but momentum is unaltered in a direct bandgap. Transition across an indirect bandgap results in the emission of heat [25]. This heat loss negatively impacts sensor operations, but is avoided with direct bandgap materials.

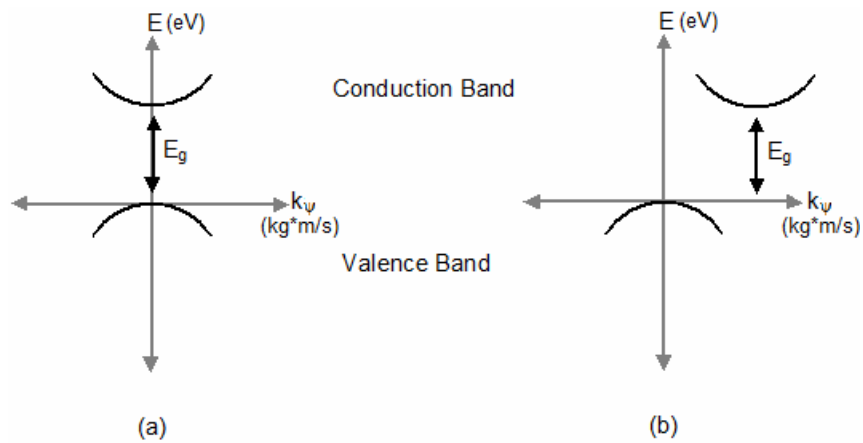


Figure 3.1: Bandgap energy transitions. a) Direct bandgap b) Indirect bandgap

### 3.1.2 Thermal stability

Sensor materials should have a high melting point to withstand high temperature operations. Hydrogen processes like SOFCs, FTS and coal gasification require operating temperatures greater than 1000 °C [2,3,26]. Sensor materials must be thermally stable under these conditions. Better thermal stability directly corresponds to a higher melting point. GaN is stable at high temperatures because the melting point of GaN is 2700 °C, which is a temperature where other semiconductors exist in the liquid phase, as shown in Table 3.2.

Table 3.2: Melting points of semiconductors. [27]

<i>Material</i>	<i>Melting Point (°C)</i>
GaN	2700
Si	937
GaAs	1421

### 3.1.3 Electron mobility

Electron mobility ( $\mu_n$ ), units  $\text{m}^2/\text{V}/\text{s}$ , relates to how sensors respond to changes in conduction of electrons or electron holes in a material. The electron drift velocity ( $v_n$ ), in  $\text{m}/\text{s}$ , is the average electron velocity caused by the application of an electric field ( $E$ ), in  $\text{V}/\text{m}$ . The movement of electrons in electron drift velocity is related to this field by the electron mobility, as shown in Equation 3.1 [24].

$$\mu_n = -\frac{E}{v_n} \quad (\text{Eqn 3.1})$$

In sensors, electron mobility should be as large as possible for better conduction without risking voltage breakdown. Breakdown occurs when a small voltage change causes a rapid current increases [28]. Semiconductors with higher  $\mu_n$  breakdown at lower voltages. Gallium nitride has average electron mobility when compared to many other semiconductors as illustrated in Table 3.3. However,  $\mu_n$  of GaN is large enough for sensor function without risking breakdown at 2.5V, which is the voltage bias for these experiments.

Table 3.3: Electron mobility of semiconductors. [25,27]

<i>Material</i>	$\mu_n (cm^2/V-s)$
GaN	440
Si	1350
SiC( $\alpha$ )	500
GaP	300
ZnS	110

### 3.2 Comparison of semiconductor sensors

Many types of hydrogen sensors utilize gallium nitride (GaN), including gate, MOS, Schottky diode and resistive sensors [6,7,29-33]. Semiconductor sensors measure an electrical property, such as resistance or capacitance which is changed due to the presence of hydrogen. Each sensor type has a distinct structure and theory of operation, despite similar sensing mechanisms. GaN resistive sensors investigated in this research operate with reduced cost and stability problems prevalent in other sensor designs.

### 3.2.1 Gate sensors

Gate sensors use platinum (Pt) or palladium (Pd) to dissociate H atoms from adsorbed H<sub>2</sub> molecules. The H atoms adsorb to the surface and then diffuse into the material between two electrodes. This diffusion changes the spacing between atoms in the material's lattice structure [34,35]. This mechanism is illustrated in Figure 3.2. Changes to the lattice alter electrical properties which corresponds to gas concentration.

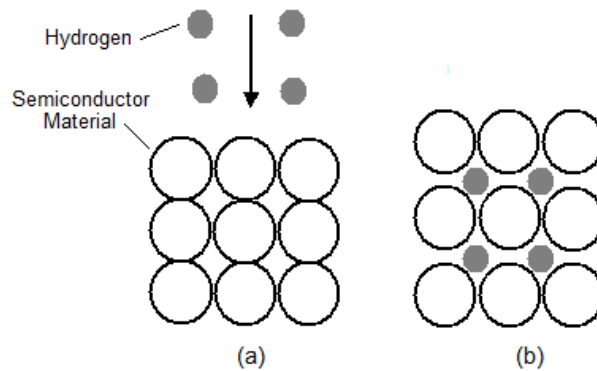


Figure 3.2: Gate sensor mechanism. a) Dissociated hydrogen atoms diffuse into the lattice. b) The presence of these atoms in the lattice changes the electrical properties of the material.

Gate sensors have some inherent design problems. Gate devices are reset by removing the hydrogen from the lattice, however some irreversible hydrogen deposition will result in hysteresis over time [22]. Also, Pt and Pd are expensive materials. Response times for gate sensors are longer because the mechanism requires diffusion of dissociated hydrogen rather than surface interactions with H<sub>2</sub> molecules.

### 3.2.2 MOS sensors

Metal-Oxide-Semiconductor (MOS) sensors were first developed by Lundstrum et al. in 1975 [36]. A metal oxide layer is deposited between a metal and semiconductor, as shown in Figure 3.3 [25,36]. The insulating oxide layer causes charge to accumulate on the metal and semiconductor layers producing a capacitive effect.

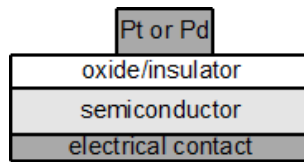


Figure 3.3: MOS sensor structure.

Similar to gate sensors, the dissociated hydrogen gas diffuses into the sensor layers. This causes a change the capacitance. Electric current is passed through the sensor by connections to electrical contacts and the catalytic metal. A voltage is applied and measured as capacitance changes, which corresponds to a certain hydrogen concentration.

MOS sensors are also hindered by many of the same issues as gate sensors, including longer response times and use of expensive metals [37]. The cost of the sensor is also increased due to the fabrication process which requires precise control of thicknesses for multiple layers.

### 3.2.3 Schottky diode sensors

In Schottky diode sensors, Pt and Pd are deposited on semiconductors such as SiC and GaN as shown in Figure3.4a [6,29-33,36]. Dissociated hydrogen diffuses through

the metal forming a layer between the metal and semiconductor (Figure 3.4b). This layer increases the potential difference between the materials, called the Schottky barrier [29]. Variations in Schottky barrier height are shown by current-voltage (I-V) characteristics which correspond to gas concentration.

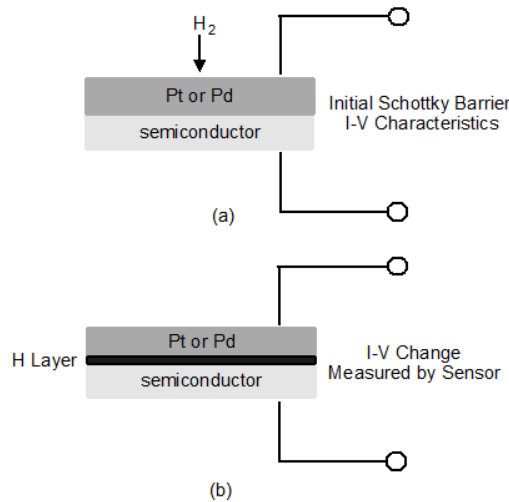


Figure 3.4: Schottky diode sensor. a)  $H_2$  dissociates on contact with catalytic metal. b) H atoms diffuse and form a layer between the metal and semiconductor, changing I-V characteristics.

A disadvantage of the Schottky diode sensors for hydrogen detection is the presence of a catalytic step to dissociate the hydrogen molecules. Thermal instability in these sensors is caused by large breakdown current leaks. Sensor structures can be modified to reduce these leaks, as decreasing dopant concentration or adding a guard ring structure [33,38,39].

### 3.2.4 Resistive sensors

Resistive gas sensors measure the change in current through the sensor under constant voltage applied across the sensor. An advantage of resistive sensors is that these electrical properties can be accurately measured. The structure of resistive sensors, shown in Figure 3.5, is a semiconductor deposited onto a substrate, such as sapphire. Metal contacts are used to induce electric charge across the semiconductor.

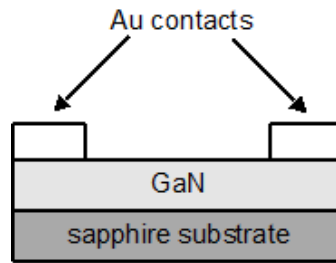


Figure 3.5: GaN resistive sensor.

The product of resistance ( $R$ ), in  $\Omega$ , and current ( $I$ ), in A, is the voltage ( $V$ ), in V, of a direct current system,  $V = IR$ . Electrical resistance depends upon the temperature of a semiconductor. Gas molecules adhere to and/or diffuse into a semiconductor. Heat transfer based on thermal interactions with  $H_2$  changes the resistance of the semiconductor [40]. A particular composition of a gas stream at a particular temperature produces a particular resistance. Thin films deposited onto the semiconductor surface increase the sensitivity of a sensor by preventing bonding of undesired species to the semiconductor surface.

There are several advantages to resistive sensors in terms of sensor construction and response. Fabrication of GaN resistive sensors is more economical than many other sensors because of inexpensive materials and a reduced number of processing steps.

Additionally, there are no catalytic metals required for sensor operations. Resistive sensor response times do not depend on diffusion into semiconductor material as in the case of other semiconductor sensors. Instead, heat transfer properties influence sensors response based on a thermal detection mechanism [40]. Changes in gas composition are detected when there is a significant difference in thermal conductivities of gas species such as between H<sub>2</sub> and N<sub>2</sub> or CO, shown in Table 2.2.

### 3.3 Summary

The properties of gallium nitride are more beneficial to sensor design than many other semiconductors, particularly silicon. GaN is thermally stable which allows devices to take advantage of bandgap characteristics at high temperatures. At these elevated temperatures, current breakdowns are less common because of GaN's moderate electron mobility.

Sensors using GaN take advantage of electrical property changes induced by exposure to a gaseous chemical system. Voltage, Schottky barrier height, and resistance are a few of the electrical properties measured by sensors to determine chemical composition. A summary comparison of common semiconductor gas sensors is shown in Table 3.4. GaN resistive sensors are able to respond faster than many other sensor types with decreased fabrication cost.

Table 3.4: Summary of semiconductor sensors.

<i>Sensor Type</i>	<i>Property Measured</i>	<i>Catalytic Metals</i>	<i>Mechanism Steps</i>
Gate Sensor	I and V	Pt/Pd	-Catalytic H <sub>2</sub> dissociation -Diffusion into semiconductor -Lattice expansion
MOS Capacitor	C and V	Pt/Pd	-Catalytic H <sub>2</sub> dissociation -Diffusion into semiconductor -Lattice expansion shifts electrical properties
Schottky Diode	I and V	Pt/Pd	-Catalytic H <sub>2</sub> dissociation -Diffusion into semiconductor -Layer of H atoms changes Schottky barrier height
Resistive Sensor	I or R	None	-H <sub>2</sub> adsorption to surface -Diffusion into semiconductor -Thermal interactions change resistance

## **Chapter 4: Experimental methods**

### 4.1 Gas sensor setup

The sensor test-bed, shown in Figure 4.1, has an automated system for data collection and control of gas flows. To initialize the sensor, a voltage is sent from the computer to the electrical housing and sensor bed. The circuit boards in the electrical housing relay information to and from the sensor. The temperature of the sensor heater is controlled in the same way with a user ramped voltage until the desired temperature is obtained. Gas flows are input by the user into a custom Labview program which controls several mass flow controllers. Gas mixtures are heated in a furnace before entering the sensor. This is done to achieve isothermal operation during experiments and minimize the effects of heat transfer between the sensor and gases. Sensor temperature, voltage and current data is collected by computer.

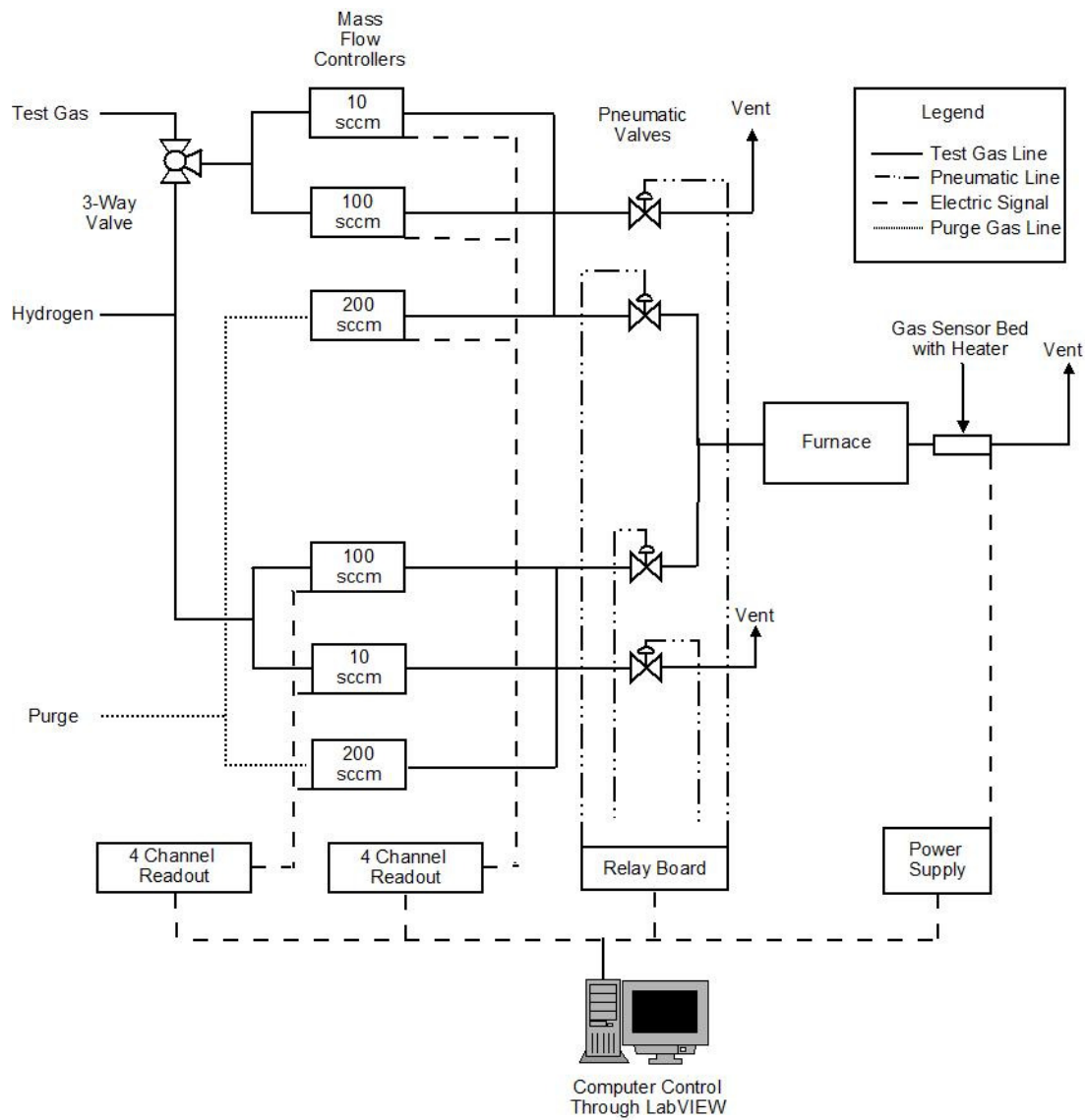


Figure 4.1: Gas sensor setup.

## 4.2 Experimental procedures

GaN resistive semiconductors were previously fabricated for testing, with silicon doped gallium nitride (n-type carrier concentration of  $2 \times 10^{18}$ ) [7]. Experiments were conducted to determine if GaN resistive sensors can detect hydrogen in nitrogen at elevated temperatures and be used to determine the H<sub>2</sub>/CO ratio of a gas stream. Nitrogen and carbon monoxide are designated carrier gases because in both cases hydrogen is the species of interest. In all experiments, sensor response to inert nitrogen (N<sub>2</sub>) at each experimental temperature was used to determine a baseline current. The voltage applied to the sensor is directly related to heat transfer between the sensor and gas streams, which affects sensitivity of the sensor [40]. Changes in the current, I (mA), across the sensor were measured under a constant voltage, V (V), of 2.5V.

As the gas mixture changes composition, the amount of heat required to keep the gas sensor at a constant temperature changes. During experimentation, voltage applied to a heater on the gas sensor was adjusted manually until the desired temperature of the sensor was reached.

The first set of experiments were conducted at 200 °C and 300 °C; pure gaseous N<sub>2</sub> and H<sub>2</sub> streams were used to establish baseline responses. Total volumetric flow rates for all of the experiments was 100 standard cubic centimeters per minute (sccm). Once isothermal conditions were met at 200 °C and 300 °C respectively, sensors were then exposed to hydrogen concentration changes in 10% steps over a range of 10-100% and in 1% steps over a range of 1-10%. Nitrogen purges to remove adsorbed H<sub>2</sub> were pulsed between changing concentrations.

In the second set of experiments, the sensor was exposed to mixtures of hydrogen and carbon monoxide with nitrogen purges between different concentrations. H<sub>2</sub>:CO ratios of 3:1, 3:2, 2:1, 1:1, 2:3 and 1:3 were tested at 50 °C. These ratios were established based on typical synthesis gas compositions used to produce different fuels for the Fischer-Tropsch synthesis [3]. Volumetric flow rate for each mixture was 100 sccm. A summary of the H<sub>2</sub>/CO concentrations and their respective gas flow rates is given in Table 4.1.

Table 4.1: H<sub>2</sub>:CO experiment flow rates.

<i>Ratio (H<sub>2</sub>:CO)</i>	<i>H<sub>2</sub> Flow Rate (sccm)</i>	<i>CO Flow Rate (sccm)</i>
3:1	75.0	25.0
2:1	66.6	33.3
3:2	60.0	40.0
1:1	50.0	50.0
2:3	40.0	60.0
1:2	33.3	66.6
1:3	25.0	75.0

## Chapter 5: Data and analysis

### 5.1 Hydrogen detection in nitrogen at 200 °C and 300 °C

The electrical response of gallium nitride (GaN) resistive sensors to increasing hydrogen concentrations in nitrogen at 200 °C and 300 °C is shown in Figure 5.1.

Current change ( $\Delta I$ ) was measured relative to the response of pure nitrogen at each temperature.  $\Delta I$  increased with an increase in hydrogen concentration.

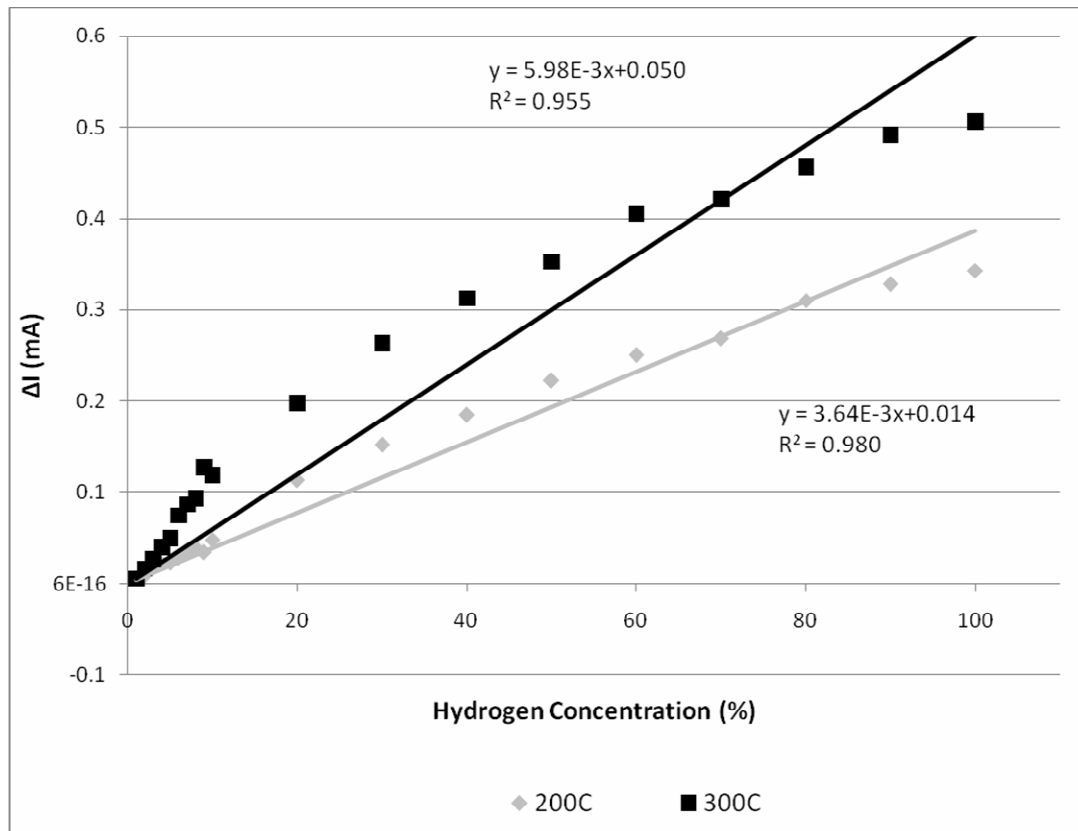


Figure 5.1: GaN sensor responses to H<sub>2</sub> in N<sub>2</sub> mixtures at 200 °C and 300 °C. Error in concentration was  $\pm 0.1\%$ .

Sensitivity analysis was performed using linear regression. Estimated sensitivity to changes in H<sub>2</sub> concentrations in N<sub>2</sub> was  $5.98 \times 10^{-3}$  mA/% H<sub>2</sub> at 300°C and  $3.86 \times 10^{-3}$  mA/% H<sub>2</sub> 200°C. This indicates that sensitivity is temperature dependent. Heat transfer between the sensor and the gas has been minimized through pre-heating of the gas. However, the sensor mechanism is affected by thermal characteristics of the gas stream [40,41]. At higher temperatures, the difference in thermal conductivities of hydrogen and nitrogen is greater which produces an increased  $\Delta I$  between concentrations.

After exposure to hydrogen, the measured sensor response to pure N<sub>2</sub> increased by 1.3%. This shift from nitrogen's original baseline value may be caused by adsorption of hydrogen. Adsorption of hydrogen is known to decrease sensitivity to changes in concentrations [42]. Such a decrease in sensitivity occurred for both high and low concentration experiments, as can be seen by slight curve in the data at higher concentrations in Figure. However, when the sensor was purged with pure nitrogen between temperature runs, sensor response returned to a linear trend, as shown in the responses to different temperatures and concentrations.

## 5.2 Sensor response to H<sub>2</sub>/CO mixtures

The response of GaN resistive sensors to various concentrations of H<sub>2</sub> in CO at 50 °C is shown in Figure 5.2. As with responses to H<sub>2</sub> in N<sub>2</sub>, the baseline for sensor current response was pure nitrogen at the experimental temperature. As with the previous test, error in concentration was  $\pm 0.1\%$ . There is a linear trend sensor response to a changing H<sub>2</sub>:CO ratio, indicating that GaN sensors are able to detect changes in H<sub>2</sub>/CO ratios.

At 300 K, thermal conductivity ( $k$ ) is  $25.0 \times 10^{-3}$  W/m/K for CO and  $25.6 \times 10^{-3}$  W/m/K for N<sub>2</sub>, whereas  $k = 186.9 \times 10^{-3}$  W/m/K for H<sub>2</sub>. [17]. Increases in H<sub>2</sub> concentration in both CO and N<sub>2</sub> follow comparable trends because the thermal characteristics of the gas mixtures are similar. The response to pure CO and pure N<sub>2</sub> gases varied less than 0.1%. Such a small difference is probably the result of similar thermal conductivities because resistive gas sensors operate on a thermal mechanism [40,41]. Sensor responses appear to show slight, if any, hydrogen adsorption, but the measured concentration span may be too small for adsorption affects to manifest.

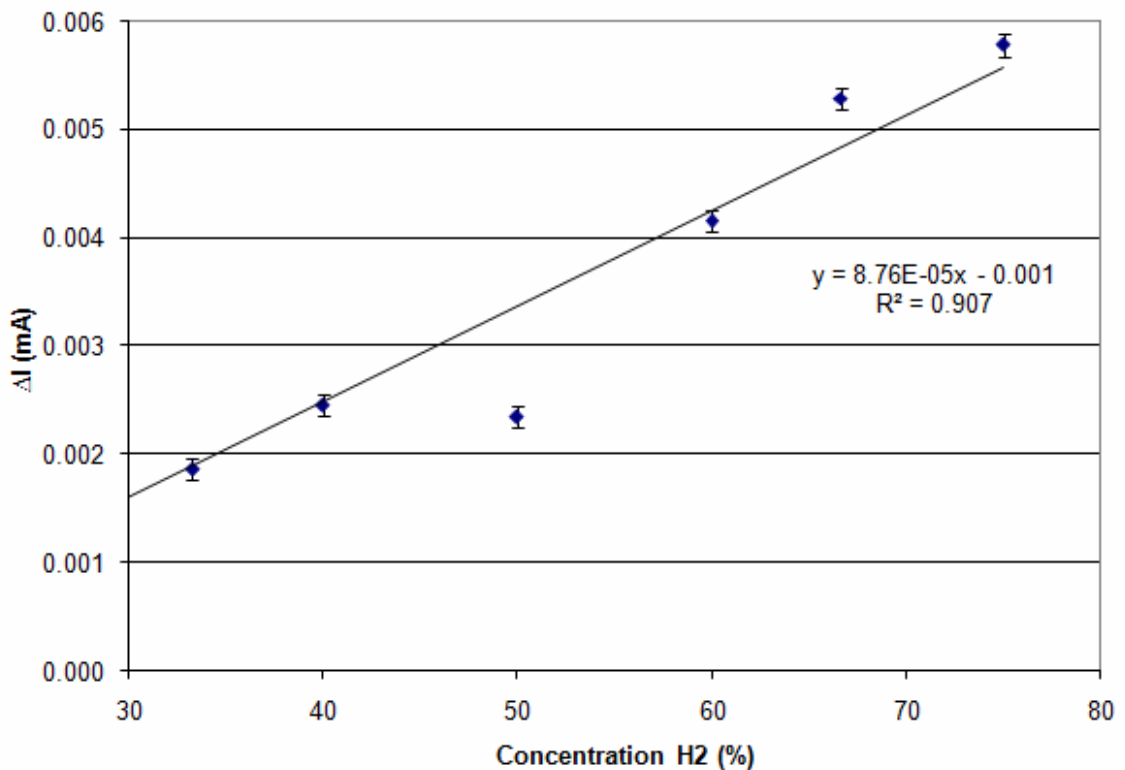


Figure 5.2: GaN sensor responses to H<sub>2</sub> in CO mixtures at 50 °C. Error in concentration was  $\pm 0.1\%$ .

Observed  $\Delta I$  measurements for H<sub>2</sub>/CO mixtures were much less than those for H<sub>2</sub>/N<sub>2</sub> mixtures. Sensitivity of H<sub>2</sub> in CO was  $8.76 \times 10^{-5}$  mA/% H<sub>2</sub>, several orders of magnitude lower than that of the higher temperature H<sub>2</sub>/N<sub>2</sub> experiments in the previous section. This could be due to the temperature dependence of resistance and sensitivity.

### 5.3 Relationship between sensor response and thermal conductivity

Previous investigations have proposed a gas sensor mechanism for resistive gas sensors [40]. Other semiconductor devices have been used as thermal conductivity detectors (TCD) utilizing a similar sensing mechanism [43,44]. Sensor data collected during for H<sub>2</sub>/N<sub>2</sub> and H<sub>2</sub>/CO mixtures has been compared to thermal conductivity to demonstrate use of GaN resistive sensors as a TCD.

Binary gas mixtures at low pressure do not follow a linear trend based upon mole fractions ( $y$ ) of gaseous species [45]. The Wassiljewa Equation with the Mason and Saxena Modification ( $A_{ij}$ ), shown below in equations 5.1 and 5.2 respectively, was used to calculate values of thermal conductivity for gas mixtures ( $k_m$ ) [45]. These equations are empirical relationships using physical properties of pure gas species, thermal conductivity ( $k$ ), molecular weight (MW) in g/mole and viscosity ( $\eta$ ) in Pa\*s.

$$k_m = \frac{\sum_{i=1}^n y_i k_i}{\sum_{j=1}^n y_j A_{ij}} \quad (\text{Eqn 5.1})$$

$$A_{ij} = \frac{\left[ 1 + \left( \frac{\eta_i}{\eta_j} \right)^{\frac{1}{2}} \left( \frac{MW_j}{MW_i} \right)^{\frac{1}{4}} \right]^2}{\left[ 8 \left( 1 + \left( \frac{MW_i}{MW_j} \right)^{\frac{1}{2}} \right) \right]} \quad (\text{Eqn 5.2})$$

TCDs compare signal response of an unknown mixture to a reference signal in the same way that sensor signals in the previous sections were referenced to the response to pure nitrogen. A model was developed for the heat balance as gas mixtures flow over the sensor using Joule's law and Newton's law of cooling. Equation 5.3 is the heat balance on the sensor where  $q$  is heat energy (in J),  $Q_{\text{heater}}$  is rate of heat transferred from the heater to the gas (in J/s),  $t$  is time (in s),  $I$  is current (in mA),  $R$  is resistance (in  $\Omega$ ),  $h$  is the heat transfer coefficient ( $\text{W}/\text{m}^2/\text{K}$ ),  $A$  is sensor surface area ( $\text{m}^2$ ), and  $\Delta T$  (in K) is difference between sensor temperature and gas temperature.

$$\frac{dq}{dt} = 10^{-6} \cdot I^2 R - h \cdot A \cdot \Delta T + Q_{\text{heater}} \quad (\text{Eqn 5.3})$$

From Ohm's law, the resistance was equivalent to the voltage divided by current. At steady state operation the change in heat energy was zero. The heat balance was then be solved for  $\Delta I(h, \Delta T)$  by subtracting the steady state balance for the reference gas from that of a particular gas concentration, which resulted in Equation 5.4. A relationship between  $h$  and  $k$  is known using the Nusselt number. However, finding  $\Delta T$  as a function of  $k$  is beyond the scope of this work. However, knowing that the relationship  $\Delta I$  theoretically exists is sufficient for analysis.

$$\Delta I = \frac{10^6}{V} (h_{gas} \cdot A \cdot \Delta T_{gas} - h_{ref} \cdot A \cdot \Delta T_{ref}) \quad (\text{Eqn 5.4})$$

Comparison of thermal conductivities to current change is shown in Figures 5.3 and 5.4. The data was suggested a power-law relationship of  $\Delta I(k)$  shown in Equation 5.5. The model fit the data with high  $R^2$  values, which supported the use of these sensors for TCD applications.

$$\Delta I \propto (k_{gas}^{1/2} - k_{ref}^{1/2}) \quad (\text{Eqn 5.5})$$

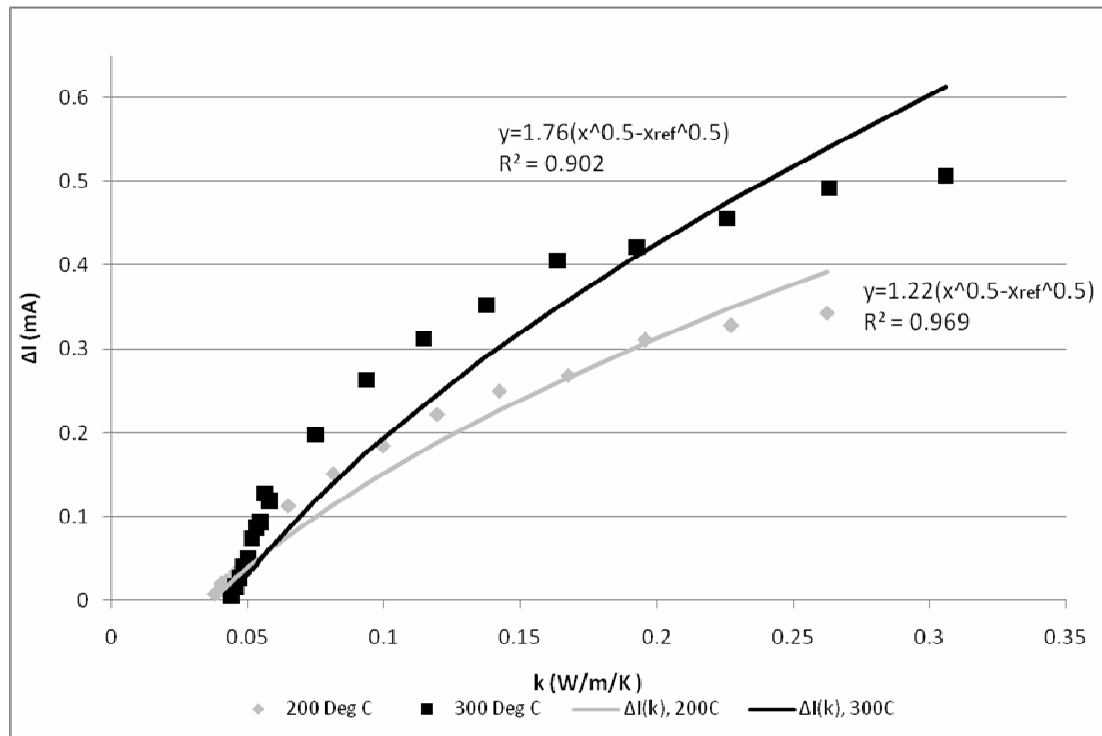


Figure 5.3: Thermal conductivity vs. current change for H<sub>2</sub> in N<sub>2</sub> mixtures.

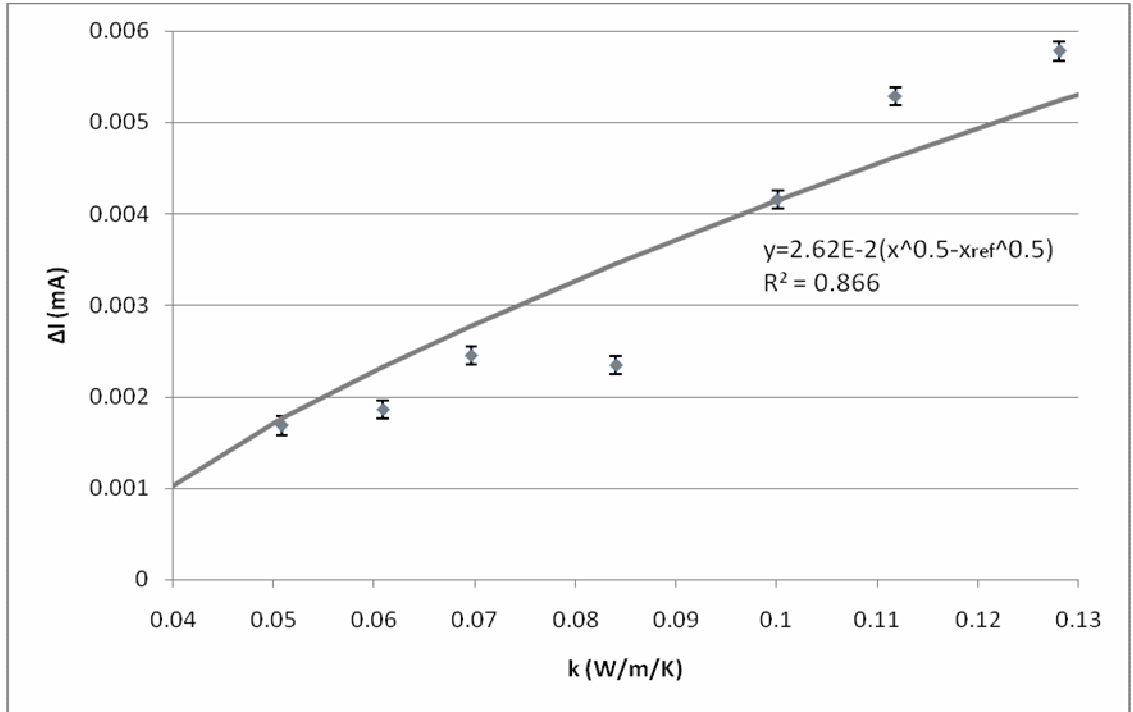


Figure 5.4: Thermal conductivity vs. current change for H<sub>2</sub> in CO mixtures at 50 °C.

#### 5.4 Summary

GaN sensors responses to H<sub>2</sub>/N<sub>2</sub> and H<sub>2</sub>/CO mixtures were observed as a direct, linear response of  $\Delta I$  to change in H<sub>2</sub> concentration in the carrier gases. Hydrogen adsorption was observed during H<sub>2</sub>/N<sub>2</sub> experiments, but was reversible with nitrogen purges. Sensor responses to pure nitrogen and carbon monoxide were equivalent. Observed sensitivity was  $5.22 \times 10^{-3}$  mA/% H<sub>2</sub> at 300°C and  $3.64 \times 10^{-3}$  mA/% H<sub>2</sub> 200°C for H<sub>2</sub>/N<sub>2</sub> mixtures and  $8.80 \times 10^{-5}$  mA/% H<sub>2</sub> for H<sub>2</sub>/CO mixtures at 50 °C. Sensor response also matches well with the empirical with empirical thermal conductivity correlations suggesting future TCD applications.

## Chapter 6: Conclusions and future work

### 6.1 Conclusions

GaN resistive sensors have been tested for gas detection. Detection of hydrogen concentrations in the presence of nitrogen was observed at temperatures up to 300 °C. Sensor response to H<sub>2</sub>/N<sub>2</sub> mixtures indicates that temperature affects sensitivity with limited changes to the reference baseline caused by H<sub>2</sub> adsorption.

Gas sensors exposure to varying ratios of H<sub>2</sub>/CO gas streams produced measureable current response to changing concentrations which was comparable to H<sub>2</sub>/N<sub>2</sub> responses. At 50 °C sensors had a clear response to changing H<sub>2</sub>/CO mixtures. However, sensitivity was much lower than that of the H<sub>2</sub>/N<sub>2</sub> mixtures which is probably caused by a reduced experimental temperature.

The sensor thermal mechanism which is utilized for gas detection is demonstrated by thermal conductivity changes. Sensor data showed a close match to the Wassiljewa Equation with the Mason and Saxena Modification for thermal conductivity. A logarithmic correlations between sensor current change and thermal conductivity was observed.

## 6.2 Future work

### 6.2.1 Further investigation into high temperature response

Testing sensor operation at temperatures above 300 °C could allow for a model of sensitivity dependence on temperature which could be used to calibrate sensors for controls of hydrogen energy processes. Selectivity to hydrogen at higher temperatures and in the presence of impurities would also be a noteworthy investigation. Impurities with similar thermal properties to hydrogen may increase current change by driving more heat transfer between the gas mixture and sensor.

### 6.2.2 Further investigation of synthesis gas sensitivity

High temperature sensor response would be an important continuation of this research. Experiments could be conducted to determine if H<sub>2</sub>/CO mixtures followed the same trend of increased sensitivity in H<sub>2</sub>/N<sub>2</sub> mixtures at higher temperatures. Elevated temperature investigations will also determine whether GaN sensors can be used in high temperature industrial processes such as FTS.

Investigations of the sensitivity of GaN sensors will also show how impurities in synthesis gas composition affect sensor response. Production of synthesis gas from coal gasification produces by products such as sulfides and carbon dioxide [26]. Irreversible adsorption or diffusion of these compounds into sensors would impact sensor response. Additional modifications to sensors may be necessary before they are practical for industrial use.

### 6.2.3 Further investigation of thermal property relationships

Measurement of physical properties of gaseous mixtures at high temperatures may be another practical application for GaN sensors. Change in thermodynamic properties and temperature dependent properties of gas mixtures other than thermal conductivity may be detectable with GaN sensors. Investigations may be conducted with correlate sensor response to properties such as gas mixture heat capacity and viscosity.

## References

- [1] A. Contreras, S. Yigit, K. Ozay, and T.N. Veziroglu, *Hydrogen as aviation fuel: A comparison with hydrocarbon fuels*, International Journal of Hydrogen Energy 22 (10-11), 1053-1060 (1997).
- [2] T.F. Fuller, and M.L. Perry, *A historical perspective of fuel cell technology in the 20<sup>th</sup> century*, Journal of the Electrochemical Society 149 (7), S59-S67 (2002).
- [3] A. Steynberg and M. Dry, *Fischer-Tropsch technology*, (Elsevier, Amsterdam, 2004).
- [4] H. Nanto, T. Minami, and S. Takata, *Zinc oxide thin film ammonia gas sensors with high sensitivity and excellent selectivity*. Journal of Applied Physics 60, 482 (1986).
- [5] S. M. Sze, *Semiconductor Sensors* (John Wiley & Sons, New York, 1994).
- [6] F.K. Yam, Z. Hassan, and A.Y. Hudeish, *The study of Pt Schottky contact on porous GaN for hydrogen sensing*, Thin Solid Films 515 (18), 7337-7341 (2007).
- [7] F. Yun, S. Chevtchenko, Y.-T Moon, H. Morkoc, T.J. Fawcett, and J.T. Wolan, *GaN resistive hydrogen gas sensors*, Applied Physics Letters 87 (7), 073507 (2005).
- [8] R.E. Krebs, *The History and Use of Our Earth's Chemical Elements*, (Greenwood Press, Westport, CT, 1998).
- [9] N.I. Sax, and R.J. Lewis, *Hawley's condensed chemical dictionary*, 11<sup>th</sup> ed., (Van Nostrand Reinhold, New York, 1987).
- [10] G.W. Hunter, P.G. Neudeck, C.C. Liu, B. Ward, Q.H. Wu, P. Dutta, M. Frank, J. Trimbol, M. Fulkerson, B. Patton, D. Makel, and V. Thomas, *Development of chemical sensor arrays for harsh environments and aerospace applications*, Sensors, 2002. Proceedings of IEEE 2, 1126-1133 (2002).

- [11] J. M. Ogden, and M.M. Steinbugler, and T. G. Kreutz, *A comparison of hydrogen, methanol and gasoline as fuels for fuel cell vehicles: implications for vehicle design and infrastructure development*, Journal of Power Sources 79, 143–168 (1999).
- [12] R. Wengenmayr, and Thomas Buhrke, *Renewable Energy*, R. Wengenmayr, Thomas Buhrke, (Wiley-vch Verlag GmbH & Co., 2008).
- [13] N. Takeichi, H. Senoh, T. Yokota, H. Tsuruta, K. Hamada, H.T. Takeshita, H. Tanaka, T. Kiyobayashi, T. Takano, and N. Kuriyama, *Hybrid hydrogen storage vessel, a novel high-pressure hydrogen storage vessel combined with hydrogen storage material*, International Journal of Hydrogen Energy 28, 1121 – 1129 (2003).
- [14] A. Lantz, J. Heffel, and C. Messer, *Hydrogen fuel cell engines and related technologies*, (College of the Desert, Palm Desert, CA, 2001).
- [15] R.B. Anderson, *The Fischer-Tropsch synthesis*, (Academic Press, Inc., Orlando 1984).
- [16] *Perry's chemical engineer's handbook*; 6<sup>th</sup> ed., edited by R. H. Perry, D. W. Green, and J. O. Maloney (McGraw-Hill, New York, 1984).
- [17] *CRC handbook of chemistry and physics*, 88<sup>th</sup> Ed., edited by D.R. Lide, (CRC Press, Boca Raton, 2008).
- [18] M. N. Carcassi, and F. Fineschi, *Deflagrations of H<sub>2</sub>-air and CH<sub>4</sub>-air lean mixtures in a vented multi-compartment environment*, Energy 30, 1439–1451 (2005).
- [19] A. Trouillet, C. Veillas, E. Sigronde, H. Gagnaire, and M. Clement, *Gaseous hydrogen leakage optical fibre detection system*, Proceedings of the SPIE – The International Society for Optical Engineering 5502 (1), 247-250 (2004).
- [20] V. Krishnan, J.W. Fergus, and F. Fasoyinu, *Solid Electrolyte Based Hydrogen Sensor for Molten Aluminum*, Advances in Aluminum Casting Technology II, edited by M. Tiryakioglu and J. Campbell (ASM International, 2002).
- [21] L. Bjornsson, E.G. Hornsten, and B. Mattiasson, *Utilization of a palladium-metal oxide semiconductor (Pd-MOS) sensor for on-line monitoring of dissolved hydrogen in anaerobic digestion*, Biotechnology and Bioengineering 73 (1), 35-43 (2001).
- [22] R.B. Gupta, *Hydrogen Fuel*, (CRC Press, Boca Raton, 2009).

- [23] O. Lenz, M. Bernhard, T. Buhrke, E. Schwartz, and B. Friedrich, *The hydrogen-sensing apparatus in Ralstonia eutropha*, Journal of Molecular Microbiology and Biotechnology, 4 (3), 255–262 (2002).
- [24] S. M. Sze, *Physics of semiconductor devices* (John Wiley & Sons, New York, 1981).
- [25] B.G. Streetman, *Solid State Electronic Devices*, 4<sup>th</sup> Ed., (Prentice-Hall, Englewood Cliffs, 1995).
- [26] C. Higman, and M. van der Burgt, *Gasification*, (Elsevier Science, New York, 2003).
- [27] <http://www.ioffe.rssi.ru/SVA/NSM/Semicond/>
- [28] R.F. Coughlin, and F.F. Driscoll, *Semiconductor Fundamentals*, (Prentice-Hall, Inc., Englewood Cliffs, 1976).
- [29] J. Schalwig, G. Muller, U. Karrer, M. Eickhoff, O. Ambacher, M. Stutzmann, L. Gorgens, and G. Dollinger, *Hydrogen response mechanism of Pt-GaN Schottky diodes*, Applied Physics Letter 80, 1222 (2002).
- [30] M. Ali, V. Cimalla, V. Lebedev, H. Romanusa, V. Tilak, D. Merfeld, P. Sandvik, and O. Ambachera, *Pt/GaN Schottky diodes for hydrogen gas sensors*, Sensors and Actuators B 113 (2), 797-804 (2006).
- [31] B. P. Luther, S. D. Wolter, and S. E. Mohny, *High temperature Pt Schottky diode gas sensors on n-type GaN*, Sensors and Actuators B: Chemical 56 (1-2), 164-168 (1999).
- [32] B.S. Kang, S. Kim, F. Ren, B.P. Gila, C.R. Abernathy, and S.J. Pearton, *Comparison of MOS and Schottky W/Pt–GaN diodes for hydrogen detection*, Sensors and Actuators B 104, 232–236 (2005).
- [33] S.W. Chunga, W.J. Hwanga, Chin C. Leeb, and M.W. Shina, *The thermal effect of GaN Schottky diode on its I-V characteristics*, Journal of Crystal Growth 268, 607–611 (2004).
- [34] K.I. Lundstrom, M.S. Shivaraman, and C.M. Svensson, *A hydrogen-sensitive Pd-gate MOS transistor*, Journal of Applied Physics 46, 3876 (1975).
- [35] L. Mariucci, A. Pecora, C. Reita, G. Petrocco, and G. Fortunato, *Pd-Gate a-Si:H thin film transistors as hydrogen sensors*, Japanese Journal of Applied Physics, 29 (12), (1990).

- [36] I. Lundstrom, S. Shivaraman, C. Svensson, and L. Lundkvist, *A hydrogen-sensitive MOS field-effect transistor*, Applied Physics Letters, 26, 55-57 (1975).
- [37] A.D. Brailsford, M. Yussouff, and E.M. Logothetis, *A first principles model of metal oxide gas sensors for measuring combustibles*, Sensors and Actuators B 49, 93-100 (1998).
- [38] R. Weiss, L. Frey and H. Ryssel, *Tungsten, nickel, and molybdenum Schottky diodes with different edge termination*, Applied Surface Science, 184 (1-4), 413-418 (2001).
- [39] S-J. Kim, S. Kim, S-J. Yu, and S-G. Kim, *Improvement in breakdown voltage characteristics of SiC Schottky barrier diode by incorporating a guard ring-assisted field limiting ring and an internal ring*, Physica Status Solidi A 203 (15), 3873-81 (2006).
- [40] T. J. Fawcett, Ph.D.Ch.E. Dissertation, University of South Florida, 2006.
- [41] T.J. Fawcett, J.T. Wolan, L. Spetz, A. Reyes, and S.E. Sadow, *Thermal detection mechanism of SiC based hydrogen resistive gas sensors*, Applied Physics Letters 89, 182102 (2006).
- [42] T. J. Fawcett, M.S.Ch.E. Thesis, University of South Florida, 2004.
- [43] P. Tardy, J.-R. Coulon, C. Lucat, and F. Menil, *Dynamic thermal conductivity sensor for gas detection*, Sensors and Actuators B 98 (1), 63-68 (2004).
- [44] G. Pollak-Diener and E. Obermeier, *Heat-conduction microsensor based on silicon technology for the analysis of two- and three-component gas mixtures*, Sensors and Actuators B 13-14 (1-3), 345-347 (1993).
- [45] B.E. Poling, J.M. Prausnitz, and J. P. O'Connell, *Properties of liquids and gases*, 5<sup>th</sup> Ed, (McGraw-Hill, New York, 2001).

## **Appendices**

## Appendix A: Nomenclature

<i>Symbol</i>	<i>Definition</i>	<i>Units</i>
A	surface area	m <sup>2</sup>
A <sub>ij</sub>	Mason-Saxena modification	dimensionless
C	concentration	moles/sscm
D <sub>AB</sub>	diffusivity in air	cm <sup>2</sup> /s
E	electric field	V/m
E <sub>g</sub>	bandgap energy	eV
h	heat transfer coefficient	W/m <sup>2</sup> /K
I	current	mA
k	thermal conductivity	W/m/K
k <sub>ψ</sub>	wave vector	kg*m/s
q	heat energy	J
Q	rate of heat transfer	J/s
R	resistance	Ω
t	time	S
T	temperature	K
v <sub>n</sub>	electron drift velocity	m/s
y	mole fraction	moles species/total moles
η	viscosity	Pa*s
μ <sub>n</sub>	electron mobility	cm <sup>2</sup> /V/s
ψ	wave function	dimensionless